MATHEMATICAL MODELS OF A NEW LUMPED-PARAMETR MAGNETOELASTIC ACCELERATION TRANSDUCER

Turayev Shovkat Dilshodovich

Senior Lecturer of the Department of "Information Technologies in Industry and Tourism" Karshi State Technical University. Adress: Uzbekistan, Karshi city, Mustakillik street 225.

E-mail: turayevshavkatxon85@gmail.com. Phone: +998902889285.

Abstract: In this article, based on the theory of lumped-parameter circuits, algebraic and differential equations describing the mechanical, electrical, and magnetic circuits of new magnetoelastic acceleration transducers, their analytical solutions, as well as mathematical models establishing the relationship between the electromotive forces at the outputs of the transducers and acceleration, which is the input quantity of the transducer, have been developed. Analysis of these mathematical models and the graphs constructed on their basis shows that under the influence of acceleration applied to the transducers, with an increase in the mechanical stresses arising in the magnetic circuit of the transducer, a redistribution of magnetic fluxes occurs between the branches of the magnetic circuit. An increase in mechanical stress leads to an increase in the magnetic flux in one branch of the magnetic circuit and a decrease in the other branch. It has been established that this is explained by the different changes in the magnetic reluctances of the corresponding parts of the magnetic core. The analysis of the graphs showed that all the considered dependences are nonlinear in nature, and the degree of this nonlinearity takes different values: if in one half of the differential magnetic circuit the degree of nonlinearity is approximately 7.93%, then in the second half of the circuit it is approximately 5.67%. The analysis of the developed mathematical models also showed that they can be used to theoretically investigate the main technical characteristics of the new acceleration transducers with sufficiently high accuracy.

Keywords: acceleration, magnetoelastic effect, magnetoelastic transducer, magnetic circuit, ferromagnetic material, equivalent substitution circuit, differential circuit, mathematical model, magnetic core, mechanical stress, magnetic flux, magnetic potential difference, magnetomotive force, magnetic reluctance, relative magnetic permeability, air gap, constraints, algebraic equation, Maclaurin series.

Introduction

Measuring and monitoring acceleration is one of the critical tasks in modern transportation, aviation, railway, energy, and industrial automatic control systems [1-3]. Especially in harsh operating conditions characterized by high temperature, strong vibration, electromagnetic interference, and moisture, the reliability and accuracy of conventional acceleration transducers decrease [4]. Consequently, interest in magnetoelastic effect-based acceleration transducers has increased in recent years. In magnetoelastic acceleration transducers (MEATs), mechanical action generates mechanical stress in ferromagnetic materials, which in turn alters their magnetic properties. As a result, the output signal is formed through changes in magnetic permeability, magnetic flux, and other parameters. These transducers are characterized by high reliability, simple design, and resistance to environmental influences [5-7].

Several new designs of MEATs have been developed at Tashkent State Transport University [8-10]. They offer advantages over existing ones due to features such as broader functional capabilities, higher sensitivity, and greater accuracy. The structure, operating principle, and specific design and electrical circuit features of these new MEATs are detailed in [8-10].

To design, fabricate, and introduce these new MEATs into production, it is first necessary to theoretically analyze their technical characteristics. The technical characteristics of MEATs primarily depend on the patterns of changes in the magnetic flux and magnetic inductions within their magnetic circuits [7]. For this purpose, it is essential to develop mathematical models for the new MEATs.

The mathematical models of the new MEATs consist of algebraic and differential equations describing their mechanical, electrical, and magnetic circuits, their analytical solutions, and expressions based on these solutions that correlate the EMF, voltage, and currents at the transducer output with the acceleration, which is the input quantity of the MEAT.

It is well known [11-14] that the excitation and measuring windings of MEATs are, in most cases, studied as electrical circuits with lumped parameters, whereas magnetic circuits are, in the vast majority of cases, analyzed as distributed-parameter circuits. However, in certain cases, particularly in rapid calculations where high computational accuracy is not strictly required, the magnetic circuits of MEATs are also investigated using the methods of lumped-parameter circuit theory [13]. In such instances, the magnetic circuits of MEATs are often described in the form of simplified equivalent circuits.

Before developing the mathematical models for the new MEATs, we introduce the following assumptions that can be adopted when investigating their electrical and magnetic circuits: 1) the active resistance of the MEAT electrical circuits is lumped and constant in value; 2) the area of the hysteresis loop of the magnetic materials used in the magnetic circuits is negligibly small for calculations; 3) the magnetic circuits operate within the linear region of the magnetization characteristic of their magnetic materials, meaning the magnetic circuit is a linear circuit; 4) the stray magnetic fluxes in the magnetic circuits have a negligibly small value that is omitted in calculations; 5) the distributed parameters of the magnetic circuits are uniformly distributed along the length of the circuit. Although these assumptions do not significantly affect the accuracy of the investigation of the new MEAT circuits, they allow for a substantial simplification of the calculations [11-12].

Figure 1a shows the design schematic of the magnetic circuit of the new MEAT [10], and Figure 1b presents its simplified equivalent circuit. The simplified nature of the equivalent circuit lies in the fact that, in the calculations, the distributed magnetic reluctances of the parallel rods of the magnetic core are replaced with lumped magnetic reluctances, and the stray magnetic fluxes merging through the air gaps between these rods are neglected. Furthermore, the circuit is assumed to be linear, meaning it is considered that the material of the transducer magnetic core operates within the linear section of the main magnetization curve.

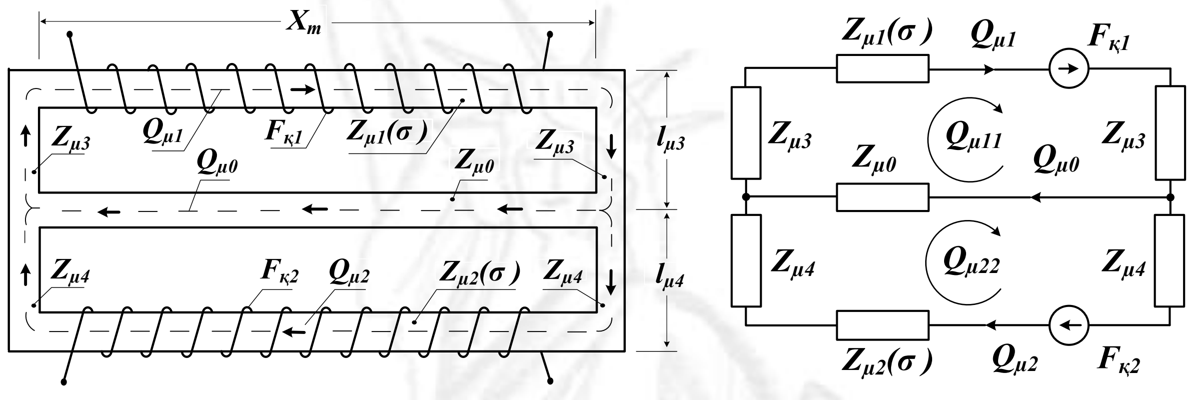

Figure 1. Design schematic (a) and simplified equivalent circuit (b) of the magnetic circuit of the new MEAT.

The mathematical model of this circuit, formulated as a system of algebraic equations using the loop (mesh) current method, is expressed as follows [15]:

$$\begin{cases} [Z_{\mu0} + Z_{\mu1}(\sigma) + 2Z_{\mu3}]Q_{\mu11} - Z_{\mu0}Q_{\mu22} = U_{\mu\kappa1}, \\ -Z_{\mu0}Q_{\mu11} + [Z_{\mu0} + Z_{\mu2}(\sigma) + 2Z_{\mu4}]Q_{\mu22} = U_{\mu\kappa2}, \end{cases} \quad (1)$$

where $Z_{\mu0} = \frac{X_м}{\mu\mu_0 bh}$ -is the total magnetic reluctance of the center rod of the magnetic core, $[H^{-1}]$; $Z_{\mu1}(\sigma) = \frac{X_м}{\mu_1(\sigma)\mu_0 bh} = \frac{d_1}{\mu_1(\sigma)}$ and $Z_{\mu2}(a) = \frac{X_м}{\mu_2(\sigma)\mu_0 bh} = \frac{d_1}{\mu_2(\sigma)}$ are the total magnetic reluctances of the upper and lower rods of the magnetic core, respectively, and $\mu_1(\sigma) = \mu(0)/(1 - C\sigma)$ and $\mu_2(\sigma) = \mu(0)/(1 + C\sigma)$ are their relative magnetic permeabilities; $\sigma = k_U U_м$ is the mechanical stress function generated in the upper and lower rods of the magnetic core by the component of the inertial force $U_м$ acting upon them; $U_м = f(a) = (\sqrt{2}/2)ma$ is the function representing the dependency of the inertial force component on acceleration a;

$Z_{\mu3} = Z_{\mu4} = \frac{l_{\mu3}}{\mu\mu_0 bh} = \frac{l_{\mu4}}{\mu\mu_0 bh}$ are the total magnetic reluctances of the left and right outer sections of the magnetic core; $X_м$; b; h; $l_{\mu3} = l_{\mu4}$ are the corresponding geometric dimensions of the magnetic circuit; $U_{\mu\kappa1}$; $U_{\mu\kappa2}$ are the MMFs (magnetomotive forces) of the excitation winding sections located on the upper and lower rods of the magnetic core. It is worth noting that in equation (1) and in most subsequent equations, complex quantities are replaced by their magnitude (modulus) values.

Based on the solution of the system of equations (1), the values of the magnetic fluxes in the respective rods of the magnetic core are equal to the following:

$$Q_{\mu 1} = Q_{\mu 11} = \frac{U_{\mu к 1} Z_{\mu 22}(\sigma) + U_{\mu к 2} Z_{\mu 0}}{Z_{\mu 11}(\sigma) Z_{\mu 22}(\sigma) - Z_{\mu 0}^2}, \quad (2)$$

$$Q_{\mu 2} = Q_{\mu 22} = \frac{U_{\mu к 1} Z_{\mu 0} + U_{\mu к 2} Z_{\mu 11}(\sigma)}{Z_{\mu 11}(\sigma) Z_{\mu 22}(\sigma) - Z_{\mu 0}^2}, \quad (3)$$

$$Q_{\mu 0} = \frac{(U_{\mu к 2} - U_{\mu к 1}) Z_{\mu 0} + [U_{\mu к 1} Z_{\mu 22}(\sigma) - U_{\mu к 2} Z_{\mu 11}(\sigma)]}{Z_{\mu 11}(\sigma) Z_{\mu 22}(\sigma) - Z_{\mu 0}^2}, \quad (4)$$

where $Z_{\mu 11}(\sigma) = Z_{\mu 0} + Z_{\mu 1}(\sigma) + 2Z_{\mu 3}$; $Z_{\mu 22}(\sigma) = Z_{\mu 0} + Z_{\mu 2}(\sigma) + 2Z_{\mu 3}$.

If the above expressions for $Z_{\mu 1}(\sigma)$, $Z_{\mu 2}(\sigma)$, $\mu_1(\sigma)$ and $\mu_2(\sigma)$ are substituted into equations (2)–(4), then after relatively simple rearrangements, we obtain the following expressions:

$$Q_{\mu 1} = \frac{U_{\mu к 1}(A_1 + B_1 \sigma) + U_{\mu к 2} Z_{\mu 0}}{A_1^2 - Z_{\mu 0}^2 - B_1^2 \sigma^2}, \quad (5)$$

$$Q_{\mu 2} = \frac{U_{\mu к 2}(A_1 - B_1 \sigma) + U_{\mu к 1} Z_{\mu 0}}{A_1^2 - Z_{\mu 0}^2 - B_1^2 \sigma^2}, \quad (6)$$

$$Q_{\mu 0} = \frac{(U_{\mu к 1} - U_{\mu к 2})(A_1 - Z_{\mu 0}) + (U_{\mu к 1} + U_{\mu к 2}) B_1 \sigma}{A_1^2 - Z_{\mu 0}^2 - B_1^2 \sigma^2}, \quad (7)$$

where $A_1 = Z_{\mu 0} + 2Z_{\mu 3} + \frac{d_1}{\mu(0)}$; $B_1 = \frac{d_1 C}{\mu(0)}$.

The graphical plots of the functions $Q_{\mu 1} = f(\sigma)$, $Q_{\mu 2} = f(\sigma)$ and $Q_{\mu 0} = f(\sigma)$ constructed according to equations (5)–(7) and their nonlinearity degrees are presented in Figure 2. These are based on the parameters of the MEAT shown in Figure 1: $U_{\mu к 1} = U_{\mu к 2} = U_{\mu к} = 300\ A$; $X_м = 0{,}1\ m$; $b = 0{,}00825\ m$; $h = 0{,}01\ m$; $d_1 = \frac{X_м}{\mu_0 bh}$; $l_{\mu 3} = 0{,}001\ m$; $\mu_0 = 4\pi \cdot 10^{-7}\ H/m$, as well as $\mu(0) = 1280$ and $C \approx 0{,}024285\ MPa^{-1}$ determined from the graphical plot of the function $\mu = f(\sigma)$ for the ferrite material reported in Figure 3.1.

An analysis of the constructed graphs shows that as the mechanical stress σ increases, the value of the magnetic flux $Q_{\mu 1}$ also increases; conversely, the value of the magnetic flux $Q_{\mu 2}$ decreases. This behavior is explained by the opposite changes in the magnetic reluctances of the respective branches of the magnetic circuit under mechanical stress, resulting from the differing variations in the magnetic permeabilities of the ferrite material from which they are made: $\mu_1(\sigma) = \mu(0)/(1 - C\sigma)$ and $\mu_2(\sigma) = \mu(0)/(1 + C\sigma)$. In turn, the value of the magnetic flux $Q_{\mu 0}$ is equal to zero when $\sigma = 0$ and subsequently increases monotonically with the increase of σ. This is attributed to the asymmetry in the distribution of magnetic fluxes across the branches of the magnetic circuit. Therefore, the quantity $Q_{\mu 0}$ can be considered an informative parameter directly related to the mechanical stress.

The graphs also indicate that within the investigated range of stresses, the dependencies $Q_{\mu1} = f(\sigma)$, $Q_{\mu2} = f(\sigma)$ and $Q_{\mu0} = f(\sigma)$ exhibit a smooth nonlinear character. However, in the region of small and medium values of σ, the variation of the magnetic fluxes is close to linear. Specifically, when the mechanical stress generated in the ferrite material under the influence of the acceleration applied to the MEAT varies within the range of $0 \le \sigma \le 40\ MPa$, the nonlinearity degrees of the function graphs for $Q_{\mu1} = f(\sigma)$, $Q_{\mu2} = f(\sigma)$ and $Q_{\mu0} = f(\sigma)$ are approximately 2.99%, 2.80%, and 2.49%, respectively. This allows for the use of linear approximation in engineering calculations and transducer sensitivity analysis. At higher values of mechanical stress, the nonlinearity becomes more pronounced, which is associated with the quadratic term $B_1^2\sigma^2$ in the denominators of the magnetic flux expressions (5)–(7).

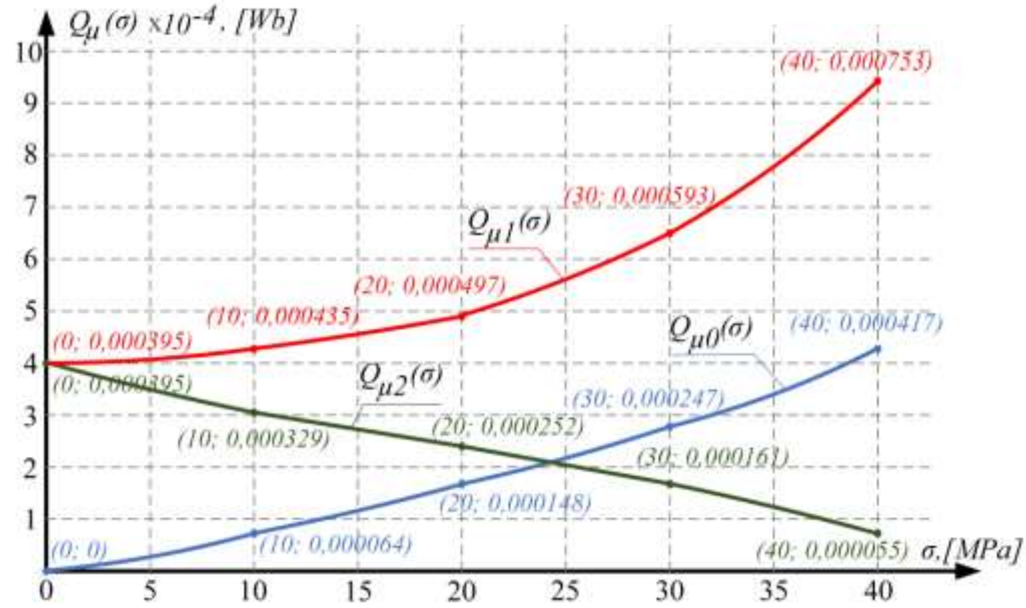

Figure 2. Graphical plots of the functions $Q_{\mu1} = f(\sigma)$, $Q_{\mu2} = f(\sigma)$ and $Q_{\mu0} = f(\sigma)$.

Thus, the obtained dependencies and constructed graphs confirm the operability of the proposed mathematical model and allow for a quantitative assessment of the effect of mechanical stress on the redistribution of magnetic fluxes in the transducer magnetic circuit.

By expanding the functions (5)–(7) into a Maclaurin series, limiting them to their first two terms, and taking into account that $\sigma = k_U U_{\text{м}}$ and $U_{\text{м}} = (\sqrt{2}/2)ma$, we obtain the following linear functions:

$$Q_{\mu1} \approx b_1 + k_1 a, \qquad (8) \qquad\qquad Q_{\mu2} \approx b_2 - k_2 a, \qquad (9)$$

$$Q_{\mu0} \approx b_0 + k_0 a, \qquad (10)$$

where

$b_1 = (U_{\mu\text{к}1}A_1 + U_{\mu\text{к}2}Z_{\mu0})/(B_1^2 - Z_{\mu0}^2)$; $\qquad k_1 = U_{\mu\text{к}1}B_1 k_U(\sqrt{2}/2)m/(B_1^2 - Z_{\mu0}^2)$;

$$b_2 = (U_{\mu\text{қ}2}A_1 + U_{\mu\text{қ}1}Z_{\mu 0})/(B_1^2 - Z_{\mu 0}^2); \qquad k_2 = U_{\mu\text{қ}2}B_1 k_U(\sqrt{2}/2)m/(B_1^2 - Z_{\mu 0}^2);$$

$$b_0 = \frac{(U_{\mu\text{қ}1} - U_{\mu\text{қ}2})(A_1 - Z_{\mu 0})}{B_1^2 - Z_{\mu 0}^2}; \qquad k_0 = \frac{(U_{\mu\text{қ}1} + U_{\mu\text{қ}2})B_1 k_U(\sqrt{2}/2)m}{B_1^2 - Z_{\mu 0}^2}.$$

The mathematical model in the form of an analytical expression for the output signal of the new MEAT, where the sections of the measuring winding are connected in a differential circuit, is equal to the following:

$$\dot{E}_{\text{чиқ.}} = j\omega w_{\text{ўлч.}}(\dot{Q}_{\mu 1} - \dot{Q}_{\mu 2}), \tag{11}$$

where $w_{\text{ўлч.}}$ and ω are the number of turns in the section of the MEAT measuring winding and the angular frequency of the current, respectively.

Figure 3 presents the design schematic (a) and the simplified equivalent circuit (b) of the magnetic circuit of the new MEAT, which converts rotational parameters, including angular acceleration, into a proportional electrical signal [9]. When this MEAT is operated in the angular acceleration measurement mode, its excitation winding is supplied by a direct current (DC) source. This current generates magnetic fluxes in the respective branches of the magnetic circuit. To determine the values of these magnetic fluxes, we formulate the following equations for the equivalent circuit in Figure 3b based on the Loop (Mesh) Current Method:

$$[W_{\mu 23} + W_{\mu 7}(\sigma) + W_{\mu 1}]Q_{\mu 11} - W_{\mu 1}Q_{\mu 22} = -U_{\mu\text{к}}, \tag{12}$$

$$-W_{\mu 1}Q_{\mu 11} + [W_{\mu 8}(\sigma) + W_{\mu 1}]Q_{\mu 22} = U_{\mu\text{к}}, \tag{13}$$

where $U_{\mu\text{к}}$ is the MMF (magnetomotive force) generated in the ferromagnetic yoke 1 by the excitation winding current; $W_{\mu 23} = W_{\mu 2} + W_{\mu 3}$; $W_{\mu 2} = W_{\mu 3} = \frac{l_{\mu\text{c}}}{\mu\mu_0 b_\text{c} h_\text{c}}$ are the magnetic reluctances of rods 2 and 3, respectively; $W_{\mu 7}(\sigma) = \frac{l_{\mu\text{x}}}{\mu_7(\sigma)\mu_0 b_\text{x} h_\text{x}} = \frac{d_2}{\mu_7(\sigma)}$; $W_{\mu 8}(\sigma) = \frac{l_{\mu\text{x}}}{\mu_8(\sigma)\mu_0 b_\text{x} h_\text{x}} = \frac{d_2}{\mu_8(\sigma)}$ are the magnetic reluctances of half-rings 7 and 8 made of magnetoelastic material;

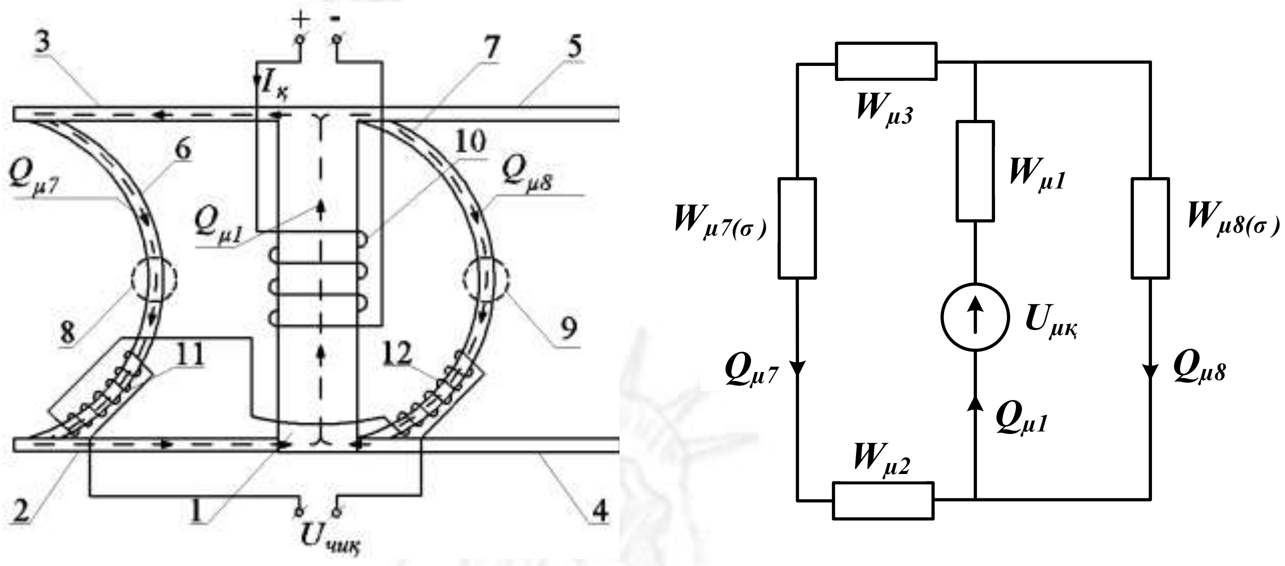

a) b)

Figure 3. Design schematic (a) and simplified equivalent circuit (b) of the magnetic circuit of the new MEAT: 1 – ferromagnetic yoke; 2–5 – rods; 6, 7 – half-rings; 8, 9 – inertial elements; 10 – excitation winding; 11, 12 – sections of the measuring winding.

$W_{\mu 1} = \frac{l_{\mu т}}{\mu \mu_0 b_т h_т}$ is the magnetic reluctance of yoke $l_{\mu с}$, $l_{\mu х}$, $l_{\mu т}$, $b_с$, $b_х$, $b_т$, $h_с$, $h_х$, $h_т$ are the length, width, and thickness of the rods, half-rings, and yoke, respectively; $\mu_7(\sigma) = \mu(0)/(1 - C\sigma)$; $\mu_8(\sigma) = \mu(0)/(1 + C\sigma)$ - are the functions representing the changes in the relative magnetic permeabilities of half-rings 7 and 8 under the influence of tensile and compressive forces, respectively; $\sigma = k_\omega \omega$ is the mechanical stress function generated in the half-rings under the action of centrifugal force as a function of the angular velocity of the inertial elements; k_ω is the proportionality coefficient.

By solving equations (12) and (13) simultaneously with respect to the unknown loop currents, we obtain the following values for the currents in the branches of the circuit:

$$Q_{\mu 1} = \frac{U_{\mu қ}[W_{\mu 23} + W_{\mu 7}(\sigma) + W_{\mu 8}(\sigma)]}{\Delta_1}, \qquad (14)$$

$$Q_{\mu 7} = \frac{U_{\mu қ} W_{\mu 8}(\sigma)}{\Delta_1}, \qquad (15)$$

$$Q_{\mu 8} = \frac{U_{\mu қ}[W_{\mu 23} + W_{\mu 7}(\sigma)]}{\Delta_1}, \qquad (16)$$

where $\Delta_1 = W_{\mu 1}[W_{\mu 23} + W_{\mu 7}(\sigma) + W_{\mu 8}(\sigma)] + [W_{\mu 23} + W_{\mu 7}(\sigma)]W_{\mu 8}(\sigma)$.

If the above expressions for $W_{\mu 7}(\sigma)$, $W_{\mu 8}(\sigma)$, $\mu_7(\sigma)$ and $\mu_8(\sigma)$ are substituted into equations (14)–(16), then after relatively simple rearrangements, we obtain the following expressions:

$$Q_{\mu 1} = \frac{U_{\mu к}\left(W_{\mu 23} + 2n\right)}{\Delta_2}, \tag{17}$$

$$Q_{\mu 7} = \frac{U_{\mu к} n(1 + C\sigma)}{\Delta_2}, \tag{18}$$

$$Q_{\mu 8} = \frac{U_{\mu к}\left[W_{\mu 23} + n(1 - C\sigma)\right]}{\Delta_2}, \tag{19}$$

where $\Delta_2 = W_{\mu 1}\left(W_{\mu 23} + 2n\right) + n\left(W_{\mu 23} + n\right) + nC\sigma W_{\mu 23} - (nC\sigma)^2$; $n = d_2/\mu(0)$.

The graphical plots of the functions $Q_{\mu 1} = f(\sigma)$, $Q_{\mu 7} = f(\sigma)$ and $Q_{\mu 8} = f(\sigma)$ constructed according to equations (17)–(19) and their nonlinearity degrees are presented in Figure 4. These are based on the parameters of the new MEAT: $l_{\mu с} = 0{,}06\, m$; $l_{\mu х} = 0{,}16\, m$; $l_{\mu т} = 0{,}1\, m$; $b_с = 0{,}005\, m$; $b_х = 0{,}005\, m$; $b_т = 0{,}01\, m$; $h_с = 0{,}005\, m$; $h_х = 0{,}005\, m$; $h_т = 0{,}005\, m$; $U_{\mu к} = 300\, A$; $\mu_0 = 4\pi \cdot 10^{-7}\ H/m$, as well as $\mu(0) = 1280$ and $C \approx 0{,}026\, MPa^{-1}$ determined from the graphical plot of the function $\mu = f(\sigma)$ for the ferrite material reported in [16].

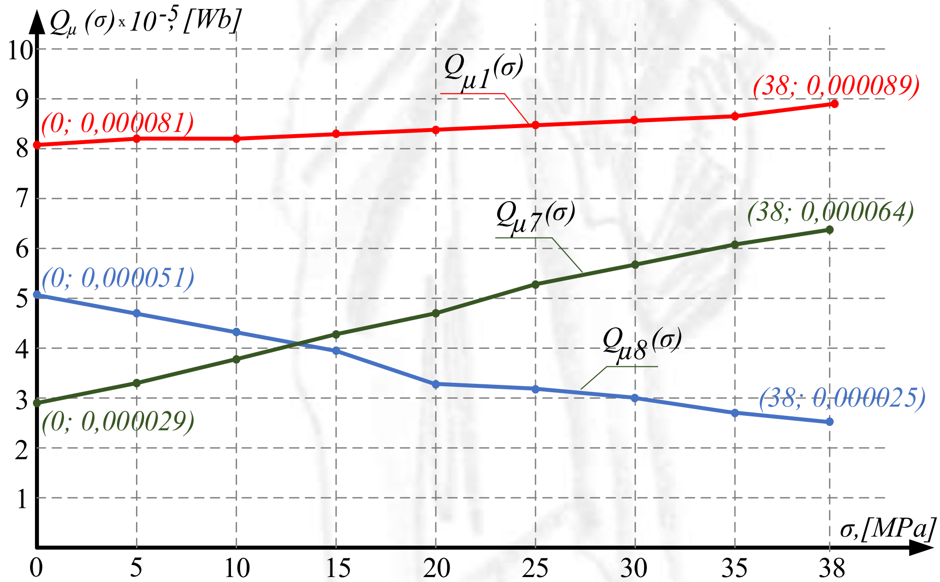

Figure 4. Graphical plots of the functions $Q_{\mu 1} = f(\sigma)$, $Q_{\mu 7} = f(\sigma)$ and $Q_{\mu 8} = f(\sigma)$ and their nonlinearity degrees.

An analysis of the obtained dependencies $Q_{\mu 1} = f(\sigma)$, $Q_{\mu 7} = f(\sigma)$ and $Q_{\mu 8} = f(\sigma)$ and their graphical plots demonstrates the redistribution of magnetic fluxes between the branches of the magnetic circuit as the mechanical stress σ increases under the influence of the acceleration applied to the MEAT. In this case, the magnetic flux $Q_{\mu 1}$ in the transducer magnetic yoke increases to a relatively lesser extent: within the mechanical stress range of $0 \leq \sigma \leq 38$, its value remains almost unchanged. An increase in mechanical stress leads to an increase in the magnetic flux in one branch of the magnetic circuit and a decrease in the other. This is explained by the differing variations in the magnetic reluctances of the respective sections of the magnetic core. The analysis of the graphs shows that all considered dependencies exhibit a nonlinear character. However, the degree of this nonlinearity varies. For the function $Q_{\mu7}(\sigma)$, the nonlinearity degree is approximately 7.93%, with the maximum deviation from the straight line connecting the points $\sigma = 0$ and $\sigma = 38$ observed at $\sigma \approx 22{,}44\ MPa$. For the function $Q_{\mu8}(\sigma)$, the nonlinearity degree is lower, equaling approximately 5.67%, and the maximum deviation occurs at $\sigma \approx 15{,}48\ \ MPa$. For the function $Q_{\mu1}(\sigma)$, the nonlinearity degree is considerably smaller, at about 1.85%, which allows it to be considered practically linear within the investigated stress range.

Thus, the function $Q_{\mu7}$ exhibits the highest sensitivity to changes in mechanical stress, while the function $Q_{\mu8}$ characterizes the variation of the magnetic flux in the opposite direction. The function $Q_{\mu1}\ (\sigma)$ serves as a practically linear reference characteristic. The obtained results confirm the validity of the adopted mathematical model and demonstrate that this magnetic circuit can be utilized to convert mechanical stress into an informative variation of magnetic fluxes.

By expanding the functions (17)–(19) into a Maclaurin series, limiting them to their first two terms, and taking into account that $\sigma = k_U U_{\text{м}}$ and $U_{\text{м}} = mr\Omega^2$ (where m - is the mass of the inertial element; r - is the distance from the axis of the ferromagnetic yoke to the center of the inertial elements; Ω is the angular velocity of the inertial elements), we obtain the following linear functions:

$$Q_{\mu1} \approx b_3 - k_3\Omega^2, \qquad (20) \qquad\qquad Q_{\mu7} \approx b_4 + k_4\Omega^2, \qquad (21)$$

$$Q_{\mu8} \approx b_5 - k_5\Omega^2, \qquad (22)$$

where

$$b_3 = U_{\mu\text{қ}}(W_{\mu23} + 2n)/\Delta_3\,; \qquad k_3 = U_{\mu\text{қ}}(W_{\mu23} + 2n)nCW_{\mu23}k_U mr/\Delta_3^2\,;$$

$$b_4 = U_{\mu\text{қ}}n/\Delta_3\,; \qquad k_4 = U_{\mu\text{қ}}nC\Delta_3^{-1}k_U mr(1 - \Delta_3^{-1}nW_{\mu23});$$

$$b_5 = U_{\mu\text{қ}}(W_{\mu23} + n)/\Delta_3\,; \qquad k_5 = U_{\mu\text{қ}}\Delta_3^{-1}nCk_U mr[1 + (W_{\mu23} + n)W_{\mu23}].$$

The resulting EMF at the output of this new MEAT, where the measuring winding sections are connected in a differential circuit, is determined using the following formula:

$$e_{\text{чиқ.}} = -w_{\text{ўлч.}}\frac{d}{dt}(Q_{\mu7} - Q_{\mu8}) = w_{\text{ўлч.}}\Omega(k_3 + k_4)\varepsilon_\Omega, \qquad (23)$$

where $\varepsilon_\Omega = \frac{d\Omega}{dt}$ – angular acceleration of the rotating part of the MEAT.

Now, we investigate the magnetic circuit of the new MEAT designed for measuring vibrational acceleration [8]. The design schematic (a) and the simplified equivalent circuit (b) of the magnetic circuit of this new MEAT are presented in Figure 5. To further simplify the investigation, the internal magnetic reluctance of the MMF sources is neglected.

In the presence of vibration along the Ox axis, to determine the magnetic fluxes in the branches of the magnetic circuit using the Loop (Mesh) Current Method, we formulate the following equations for the independent loops "$oaa'o'o$", "$odd'o'o$", "$obb'o'o$" and "$occ'o'o$":

$$[Z_{\mu0} + Z_{\mu1}(\sigma)]Q_{\mu11} + Z_{\mu0}Q_{\mu22} - Z_{\mu0}Q_{\mu33} - Z_{\mu0}Q_{\mu44} = 2U_{\mu\kappa}, \quad (24)$$
$$Z_{\mu0}Q_{\mu11} + [Z_{\mu0} + Z_{\mu1}(\sigma)]Q_{\mu22} - Z_{\mu0}Q_{\mu33} - Z_{\mu0}Q_{\mu44} = 2U_{\mu\kappa}, \quad (25)$$
$$-Z_{\mu0}Q_{\mu11} - Z_{\mu0}Q_{\mu22} + [Z_{\mu0} + Z_{\mu2}(\sigma)]Q_{\mu33} + Z_{\mu0}Q_{\mu44} = 2U_{\mu\kappa}, \quad (26)$$
$$-Z_{\mu0}Q_{\mu11} - Z_{\mu0}Q_{\mu22} + Z_{\mu0}Q_{\mu33} + [Z_{\mu0} + Z_{\mu2}(\sigma)]Q_{\mu44} = 2U_{\mu\kappa}, \quad (27)$$

where $Z_{\mu0} = \frac{l_{\mu c}}{\mu\mu_0 bh}$ is the total magnetic reluctance of the additional rod (branch oo' in Figure 5b) in the transducer magnetic circuit (when the transducer magnetic system attached to the monitored object undergoes oscillatory motion at a certain frequency, eddy currents are generated in the rods due to the regular variation of their magnetic fluxes over time; therefore, the magnetic reluctances of the rods are considered in the form of total reluctance); $Z_{\mu1}(\sigma) = \frac{d_3}{\mu_1(\sigma)}$, $Z_{\mu2}(\sigma) = \frac{d_3}{\mu_2(\sigma)}$ – are the total magnetic reluctances of the main rods (branches (aa', dd' and bb, cc' in the transducer magnetic circuit; $d_3 = l_{\mu c}/(\mu_1 bh)$; $Q_{\mu11} \div Q_{\mu44}$ – are the magnetic fluxes of the independent loops of the magnetic circuit.

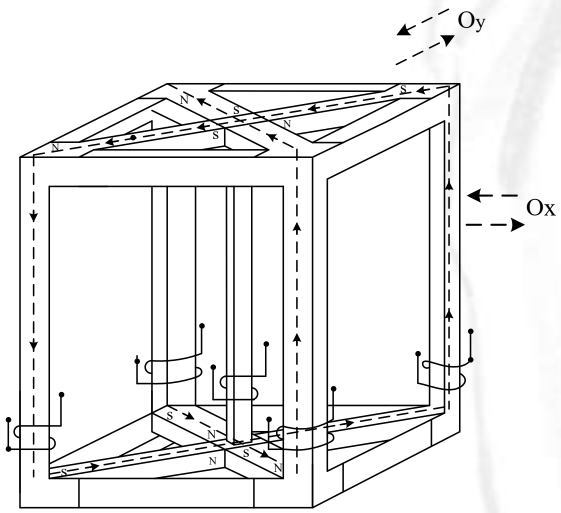

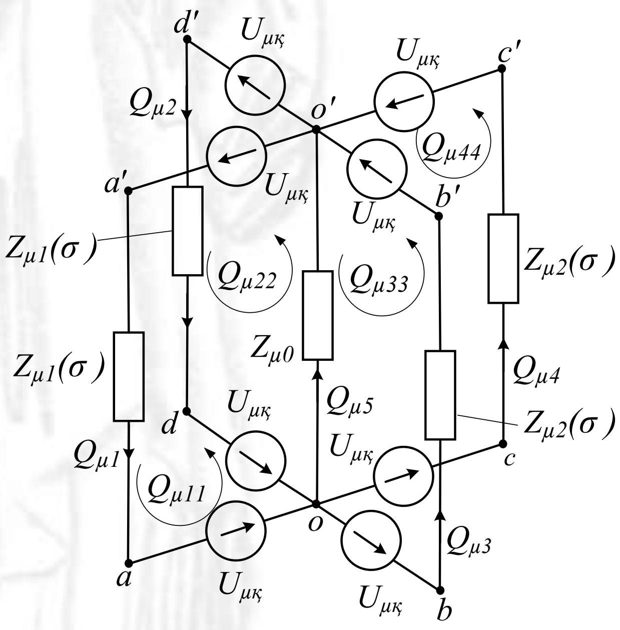

Figure 5. Design schematic (a) and simplified equivalent circuit (b) of the magnetic circuit of the new MEAT designed for measuring vibrational acceleration.

By solving the algebraic equations (24)–(27) simultaneously with respect to the loop magnetic fluxes, we obtain the following expressions for the magnetic fluxes merging through the branches based on them:

$$Q_{\mu 1} = Q_{\mu 2} = \frac{2U_{\mu\kappa}\left[4Z_{\mu 0} + Z_{\mu 2}(\sigma)\right]}{2Z_{\mu 0}\left[Z_{\mu 1}(\sigma) + Z_{\mu 2}(\sigma)\right] + Z_{\mu 1}(\sigma)Z_{\mu 2}(\sigma)}, \tag{28}$$

$$Q_{\mu 3} = Q_{\mu 4} = \frac{2U_{\mu\kappa}\left[4Z_{\mu 0} + Z_{\mu 1}(\sigma)\right]}{2Z_{\mu 0}\left[Z_{\mu 1}(\sigma) + Z_{\mu 2}(\sigma)\right] + Z_{\mu 1}(\sigma)Z_{\mu 2}(\sigma)}, \tag{29}$$

$$Q_{\mu 5} = \frac{4U_{\mu\kappa}\left[Z_{\mu 2}(\sigma) - Z_{\mu 1}(\sigma)\right]}{2Z_{\mu 0}\left[Z_{\mu 1}(\sigma) + Z_{\mu 2}(\sigma)\right] + Z_{\mu 1}(\sigma)Z_{\mu 2}(\sigma)}. \tag{30}$$

When a force acts on the magnetic core from left to right along the direction of the Ox axis, the branches bb' and cc' (main rods) of the magnetic core experience tensile stress, whereas the branches aa', dd' (main rods) experience compressive stress. In this case, the values of the relative magnetic permeability of the rods bb' and cc' vary according to the law $\mu_1(\sigma) = \mu(0)/(1 - C\sigma)$, and those of the rods aa' and dd' vary according to the law $\mu_2(\sigma) = \mu(0)/(1 + C\sigma)$. Here, it should be noted that the variations of μ under tension and compression for the magnetoelastic rods are, by convention, assumed to be mutually equal.

Substituting the expressions for $Z_{\mu 1}(\sigma)$, $Z_{\mu 2}(\sigma)$, $\mu_1(\sigma)$ and $\mu_2(\sigma)$ into equations (28)–(30), we obtain the following:

$$Q_{\mu 1} = Q_{\mu 2} = \frac{2U_{\mu\kappa}\mu(0)\left[4Z_{\mu 0}\mu(0) + d_3(1 + C\sigma)\right]}{d_3\left[4Z_{\mu 0}\mu(0) + d_3(1 - C^2\sigma^2)\right]}, \tag{31}$$

$$Q_{\mu 3} = Q_{\mu 4} = \frac{2U_{\mu\kappa}\mu(0)\left[4Z_{\mu 0}\mu(0) + d_3(1 - C\sigma)\right]}{d_3\left[4Z_{\mu 0}\mu(0) + d_3(1 - C^2\sigma^2)\right]}, \tag{32}$$

$$Q_{\mu 5} = \frac{8U_{\mu\kappa}\mu(0)C\sigma}{d_3\left[4Z_{\mu 0}\mu(0) + d_3(1 - C^2\sigma^2)\right]}, \tag{33}$$

The graphical plots of the functions $Q_{\mu 1} = Q_{\mu 2} = f(\sigma)$, $Q_{\mu 3} = Q_{\mu 4} = f(\sigma)$ and $Q_{\mu 5} = f(\sigma)$ constructed according to equations (31)–(33) and their nonlinearity degrees are presented in Figure 6. These are based on the parameters of the MEAT shown in Figure 5: $l_{\mu c} = 0{,}1\ m$; $b = 0{,}005\ m$; $h = 0{,}005\ m$; $U_{\mu\kappa} = 300\ A$; $\mu_0 = 4\pi \cdot 10^{-7}\ H/m$, as well as $\mu(0) = 1280$ and $C \approx 0{,}026\ MPa^{-1}$ determined from the graphical plot of the function $\mu = f(\sigma)$ for the ferrite material reported in [16].

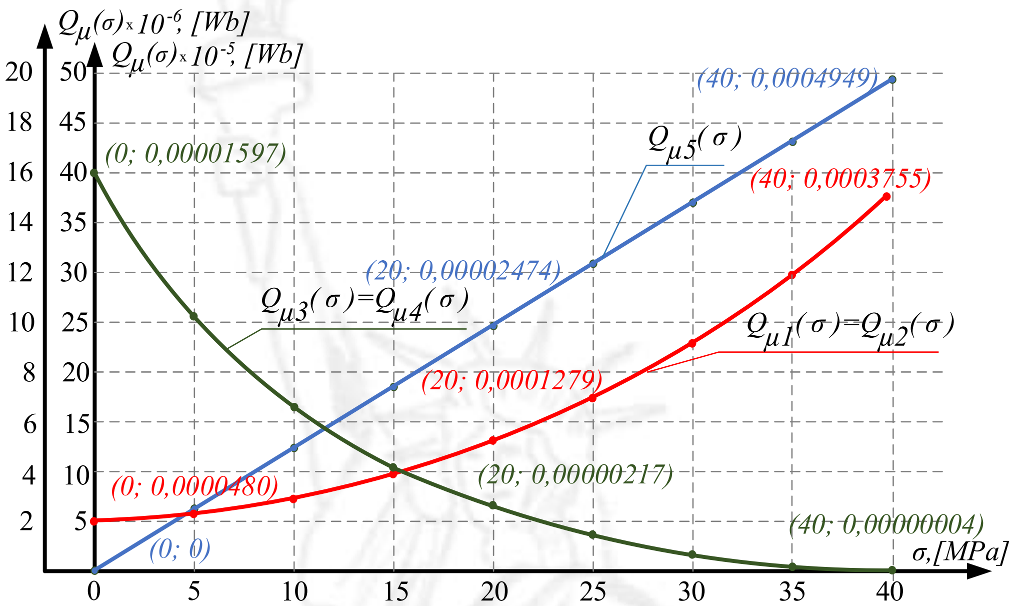

Figure 6. Graphical plots of the functions $Q_{\mu 1} = Q_{\mu 2} = f(\sigma)$, $Q_{\mu 3} = Q_{\mu 4} = f(\sigma)$ and $Q_{\mu 5} = f(\sigma)$.

Based on the derived analytical expressions for the working magnetic fluxes in the main and additional rods of the new MEAT and the graphs constructed from them, the following scientific conclusions can be formulated: 1) the functions $Q_{\mu 1}(\sigma) = Q_{\mu 2}(\sigma)$, $Q_{\mu 3}(\sigma) = Q_{\mu 4}(\sigma)$ and $Q_{\mu 5}(\sigma)$ and their graphs confirm that the mechanical stress σ exerts a significant influence on the redistribution of magnetic fluxes within the magnetic circuit; 2) as σ increases, the flux $Q_{\mu 1}(\sigma) = Q_{\mu 2}(\sigma)$ increases, the flux $Q_{\mu 3}(\sigma) = Q_{\mu 4}(\sigma)$ decreases, and the flux $Q_{\mu 5}(\sigma)$ increases monotonically starting from a zero value; 3) under the influence of mechanical stress, the magnetic reluctances in the branches of the magnetic circuit vary differently: magnetic permeability increases in some branches and decreases in others, resulting in a redistribution of magnetic fluxes between the symmetrical sections of the magnetic circuit; 4) the function $Q_{\mu 5}(\sigma)$ possesses the most distinct measurement capability since its value is zero at $\sigma = 0$ and increases with the growth of σ, meaning this flux can be utilized as the informative output parameter of the transducer; 5) the graphical plot of the function $Q_{\mu 5}(\sigma)$ exhibits the lowest degree of nonlinearity, which is crucial because this specific function is the most optimal for forming a measurement signal with minimal nonlinearity error; 6) the obtained formulas and graphs confirm the feasibility of applying the investigated new MEAT to convert mechanical stress into an electrical signal based on the magnetoelastic effect, and demonstrate that it is expedient to adopt the function (magnetic flux) $Q_{\mu 5}(\sigma)$ as the primary informative parameter.

If the resulting functions (31)–(33) are expanded into a Maclaurin series, limiting them to their first two terms, and taking into account the relations $\sigma = k_U U_{м}$ and $U_{м} =$

$mA_m sin(\omega_м t)$ (where A_m, $\omega_м$ – are the amplitude and angular frequency of the vibrational acceleration, respectively), then we obtain the following linear expressions for the magnetic fluxes in the respective branches of the transducer magnetic circuit:

$$Q_{\mu 1} \approx b_6 + k_6 A_m sin(\omega_м t), \quad (34) \qquad Q_{\mu 3} \approx b_6 - k_6 A_m sin(\omega_м t), \quad (35)$$

$$Q_{\mu 5} \approx 4k_6 A_m sin(\omega_м t), \quad (36)$$

where $b_6 = 2U_{\mu к}\mu(0)/d_3$; $k_6 = 2U_{\mu к}\mu(0)Cm/\left(4Z_{\mu 0}\mu(0) + d_3\right)$.

The EMFs induced in the main and additional measuring windings of the new MEAT proportionally to the vibrational acceleration are determined using the following expressions:

$$e_{ac.} = -2w_{ac.}\left(\frac{dQ_{\mu 1}}{dt} - \frac{dQ_{\mu 3}}{dt}\right) = -4w_{ac.}k_6\omega_м A_m cos(\omega_м t), \quad (37)$$

$$e_{қўш.} = -w_{қўш.}\frac{dQ_{\mu 5}}{dt} = -w_{қўш.}k_6\omega_м A_m cos(\omega_м t). \quad (38)$$

Conclusion.

Thus, in this paper, based on the theory of lumped-parameter circuits, mathematical models for the new MEATs have been developed. These models include algebraic and differential equations describing the mechanical, electrical, and magnetic circuits, their analytical solutions, and expressions derived from these solutions that correlate the EMFs at the transducer output with the acceleration, which is the input quantity of the MEAT. An analysis of these mathematical models and the graphs constructed from them demonstrates the redistribution of magnetic fluxes between the branches of the magnetic circuit as the mechanical stress σ increases under the influence of the acceleration applied to the MEAT. It was determined that an increase in mechanical stress leads to an increase in the magnetic flux in one branch of the magnetic circuit and a decrease in the other, which is explained by the differing variations in the magnetic reluctances of the respective sections of the magnetic core. The analysis of the graphs showed that all considered dependencies exhibit a nonlinear character and that the degrees of these nonlinearities vary. Specifically, while the nonlinearity degree in one half-section of the differential magnetic circuit is approximately 7.93%, it equals about 5.67% in the second half-section of the circuit.

References:

1. Kabanov V.N. Elementy avtomatiki: ucheb. posobiye / V.N. Kabanov. – Yekaterinburg: Uralskiy gosudarstvennyy universitet putey soobshcheniya, 2010. – 187 s.
2. Yusupbekov N.R., Igamberdiyev X.Z., Malikov A.V. Osnovy avtomatizatsii texnologicheskix protsessov: Uchebnoye posobiye dlya vysshego i srednego spetsialnogo obrazovaniya. V 2-x ch. – T.: TGTU, 2007. Ch.1, 2. – 152 s.
3. Shandrov B.V. Texnicheskiye sredstva avtomatizatsii: uchebnik dlya studentov vysshix uchebnyx zavedeniy / B.V. Shandrov, A.D. Chudakov. – Moskva: Izdatelskiy tsentr «Akademiya», 2007. – 368 s.

4. Frayden Dj. Sovremennyye datchiki. Spravochnik. Seriya: Mir elektroniki. – Moskva: Texnosfera, 2005. – 592 s.
5. S. R. Green, Y.B. Gianchandani Wireless Magnetoelastic Transducers for Biomedical Applications Center for Wireless Integrated MicroSensing and Systems (WIMS2) University of Michigan, Ann Arbor, MI 48109, pp. 1226–1233, May 2012.
6. Jadobin N.Ye., Lebedev A.I. Magnitouprugiye preobrazovateli v SEU // Transport Rossiyskoy Federatsii. – Moskva, 2006. – №6. – S. 36–38.
7. Amirov S.F., Jurayeva K.K. Magnitouprugiye datchiki usiliy dlya sistem kontrolya i upravleniya obyektami jeleznodorojnogo transporta // Monografiya. Izdatelstvo «Fan va texnologiya», Toshkent, 2019. – 162 s.
8. Patent RUz (UZ) № IAP 7870. Magnitouprugiy preobrazovatel dlya izmereniya parametrov vibratsii / Amirov S.F., Jurayeva K.K., Fayzullayev J.S., Turayev Sh.D., 2024, Byulleten izobreteniy № 11.
9. Patent RUz (UZ) № IAP 7878. Magnitouprugiy preobrazovatel parametrov vrashcheniya / Amirov S.F., Jurayeva K.K., Fayzullayev J.S., Turayev Sh.D., 2024, Byulleten izobreteniy № 12.
10. Patent RUz (UZ) № IAP 8155. Magnitouprugiy preobrazovatel uskoreniy / Amirov S.F., Fayzullayev J.S., Jurayeva K.K., Turayev Sh.D., 2025, Byulleten izobreteniy №.
11. Zaripov M.F. Preobrazovateli s raspredelennymi parametrami dlya avtomatiki i informatsionno-izmeritelnoy texniki. – Moskva: Energiya, 1969. – 176 s.
12. Konyuxov N.Ye. i dr. Elektromagnitnyye datchiki mexanicheskix velichin / N.Ye. Konyuxov, F.M. Mednikov, M.L. Nechayevskiy. – Moskva: Mashinostroyeniye, 1987. – 256 s.
13. Fedotov A.V. Teoriya i raschet induktivnyx datchikov peremeshcheniy dlya sistem avtomaticheskogo kontrolya: monografiya. – Omsk: Izd-vo OmGTU, 2011. – 176 s.
14. Plaxtiyev A.M. Beskontaktnyye ferromagnitnyye preobrazovateli s raspredelennymi magnitnymi parametrami dlya sistem kontrolya i upravleniya: Dis. … dokt. texn. nauk. – Toshkent: ToshGTU, 2009. – 399 s.
15. Demirchyan K.S., Neyman L.R., Korovkin N.V., Chechurin V.L. Teoreticheskiye osnovy elektrotexniki: V 3-x t. Uchebnik dlya vuzov. Izd. 4-ye. – Sankt-Peterburg: Piter, 2006, tom 1. – 464 s.
16. S. R. Green, Y.B. Gianchandani Wireless Magnetoelastic Transducers for Biomedical Applications Center for Wireless Integrated MicroSensing and Systems (WIMS2) University of Michigan, Ann Arbor, MI 48109, pp. 1226–1233, May 2012.